Saudi Pharmaceutical Journal 28 (2020) 719–728

Contents lists available at ScienceDirect

Saudi Pharmaceutical Journal

journal homepage: www.sciencedirect.com

Original article

Design of expert guided investigation of native L-asparaginase encapsulated long-acting cross-linker-free poly (lactic-co-glycolic) acid nanoformulation in an Ehrlich ascites tumor model

Manvi Singh [a], Nazia Hassan [a], Devina Verma [a], Pragya Thakur [a], Bibhu Prasad Panda [b], Amulya Kumar Panda [c], Rakesh Kumar Sharma [d], Aamir Mirza [a], Sheikh Mansoor [e], Salman H. Alrokayan [f], Haseeb A. Khan [f], Parvaiz Ahmad [g], Zeenat Iqbal [a,*]

[a] Department of Pharmaceutics, School of Pharmaceutical Education and Research, Jamia Hamdard, New Delhi, Delhi 110062, India
[b] Microbial and Pharmaceutical Biotechnology Laboratory, Jamia Hamdard, New Delhi 110062, India
[c] Product Development Cell, National Institute of Immunology, Aruna Asaf Ali Marg, New Delhi 110067, India
[d] Division of Radiopharmaceuticals and Radiation Biology, Institute of Nuclear Medicine and Allied Sciences, Brig. SK Mazumdar Road, Delhi 110 054, India
[e] Division of Biochemistry, SKUAST, Jammu 180009, India
[f] Department of Biochemistry, College of Science, King Saudi University, P.O. Box. 2455, Riyadh 11451, Saudi Arabia
[g] Botany and Microbiology Department, College of Science, King Saudi University, P.O. Box. 2460, Riyadh 11451, Saudi Arabia

ARTICLE INFO

Article history:
Received 2 January 2020
Accepted 28 April 2020
Available online 6 May 2020

Keywords:
Chemotherapy
PLGA
L-asparaginase
Box-Behnken Design
Ehrlich ascites tumor (EAT) model
Tumor volume

ABSTRACT

Present study explores native L-asparaginase encapsulated long-acting cross-linker-free PLGA-nanoformulation in an Ehrlich ascites tumor model. L-asparaginase-PLGA nanoparticles for tumor were prepared using a double emulsion solvent evaporation technique, optimized and validated by Box-Behnken Design. L-ASN-PNs showed a particle size of 195 nm ± 0.2 nm and a PDI of 0.2. Scanning Electron Microscopy (SEM) and Transmission Electron Microscopy (TEM) techniques revealed its smooth morphology and elicited an *in-vitro* release of 80% of the drug, following the Higuchi drug release model. *In-vivo* studies of L-ASN-PNs on an Ehrlich ascites tumor (EAT) model were completed and compared with the standard medication of 5-fluorouracil (5-FU) treatment. L-ASN-PN treated mice showed a 51.15% decrease in tumor volume and 100% survival rate with no reduction in body weight, no haemotoxicity and no hepatotoxicity, as evident from the hematological parameters, and liver enzyme parameters that were well within the prescribed limits. Chemotherapy has severe side effects and restricted therapeutic success. Henceforth, the purported L-Asparaginase PLGA nanoparticles are a suitable entity for better tumor regression, intra-tumor accumulation and no hematological side-effects.

1. Introduction

One of the viable options for the treatment of acute lymphoblastic leukaemia (ALL) is the enzyme L-asparaginase. It is known to cause destruction of asparagine-dependent tumors by degrading the circulating L-asparagine (Brambilla et al., 1970; Pieters et al., 2010). However, use of L-asparaginase is associated with allergic reactions as side effects. The half-life of circulating L-asparaginase is drastically reduced (from 18 to 24 h to approximately 2.5 h) due to the systemic emergence of neutralizing antibodies (Bahreini et al., 2014) proteolytic degradation of circulating L-asparaginase by the proteases of the host organism is also responsible for the shorter half-life. Apart from the drawback of a very short half-life, it is known to elicit its effects against leukaemia only in the tetrameric form (Bahreini et al., 2014). Therefore, researchers working in the field of L-asparaginase focus on ways to circumvent these side effects along with techniques to improve its half-life *in-vivo*. The most popular approach, which has yielded satisfactory results, has been the chemical modification of asparaginase by covalently bonding the enzyme with polyethylene glycol (Matsushima et al., 1980) or poly-(D, L-alanine) (Uren et al., 1982) or dextran (Wileman et al., 1986). The current standard-of-care

* Corresponding author.
E-mail address: zeenatiqbal@jamiahamdard.ac.in (Z. Iqbal).
Peer review under responsibility of King Saud University.

Production and hosting by Elsevier

https://doi.org/10.1016/j.jsps.2020.04.014
1319-0164/

formulation is L-asparaginase, obtained from E. coli, (Moola et al., 1994; Jain et al., 2012, Cedar and Schwartz, 1968) covalently conjugated to polyethylene glycol (PEG) for extended circulation half-life and protection from immune responses. In addition to allergic reactions, treatment with this standard of care is also riddled with L-asparaginase's incapacitating effect on the haematopoietic and hepatic systems, which can cause easy bleeding, unusual anaemia and jaundice (Moola et al., 1994). The risk of severe immune reactions and other haematopoietic side effects, has confined L-asparaginase therapy to ALL, regardless of increasing *in-vitro* evidence showing that other cancers might be sensitive to asparagine depletion and hence, L-asparaginase treatment as well (Masetti and Pession, 2009). Furthermore, both asparaginase and pegasparase, another protein drug, results in hepatotoxicity and consequently, a decrease in serum albumin and clotting factors and an increase in alkaline phosphatase, serum aminotransferase and bilirubin levels (Masetti and Pession, 2009). This hepatotoxicity may be transformed into a more severe and protracted form of liver injury, which may be marked by fatigue, dark urine and jaundice. In addition, native asparaginase causes moderate to severe anorexia and coagulopathy leading to bleeding or thrombotic events such as stroke (Fu and Sakamoto, 2007).

To counter the pitfalls of L-asparaginase, researchers have explored immobilization of the enzyme using nanotechnological preparations. These formulations have been designed to gain better thermal and pH stability, resist proteases and decrease the side effects caused by the release of a native enzyme in systemic circulation. L-asparaginase nanoformulations have been prepared as liposomes (Fishman and Citri, 1975), poly(D,L-lactide-co-glycolide) (PLG) nanoparticles (Gaspar et al., 1998), and hydrogel-magnetic nanoparticles (Teodor et al., 2009).

Various groups have worked on strategies to develop asparaginase-conjugated nanoparticles and studies have revealed that L-asparaginase was encapsulated in PLG nanospheres and found that high-molecular-weight PLG nanospheres showed larger size, higher loading and slower release rates when compared with low-molecular-weight PLG nanospheres (Gaspar et al., 1998). However, even with this inference, the best drug loading obtained was a meagre 4.86%, and the side effects profile was not much different from the existing one (Gaspar et al., 1998). Meanwhile, PLGA nanoparticle using polyvinyl alcohol (PVA) as emulsifier were formed. Owing to the higher hydrophilicity of the nanoparticle surface, more residual PVA on the nanoparticles was observed, resulting in lower intracellular uptake (Wang et al., 1999). Additionally, L-asparaginase-loaded poly(D,L-lactide-co-glycolide) nanospheres were prepared using various stabilizers and uncovered the fact that the enzyme is denatured at the aqueous/organic interface due to sonication (Wolf et al., 2003). Additionally, after lyophilization, the enzyme activity and particle size distribution were retained only by use of Pluronic F68 as lyoprotectant. In spite of maintaining unaltered particle size and improved biological activity, the release profile of the enzyme was strongly altered by co-encapsulation of the stabilizers, resulting in increased first bursts (Wolf et al., 2003). A nano-biocomposite of zinc oxide nanoparticles conjugated with L-asparaginase were developed. However, the enzyme that could be used to prepare these particles was derived from *Aspergillus terreus*, which is less active than the enzyme derived from bacterial origin (Wolf et al., 2003). Further, zinc oxide nano-biocomposites of fungal asparaginase conjugated to colloidal magnetic nanoparticles were developed. Nevertheless, it was necessary to use glutaraldehyde pre-treatment for the development of this nanoformulation (Baskar et al., 2015). Therefore, we perceived that this strategy of producing a safe effective formulation of L-asparaginase for use in not just ALL but in other responsive cancers too is embedded with problems in the form of restrictive drug loading in a nanocarrier, use of toxic cross-linking agents such as glutaraldehyde and glucomannan and a decrease in enzyme activity due to denaturation in the preparation process as well as during covalent coupling of the nanocarrier to the enzyme. Thus, this presents a rationale for delevoping L-asparaginase nano-delivery system for cancer treatment that would effectively mitigate the side effects associated with intravenous administration of L-asparaginase, as well as overcome the formulation challenges.

Polymeric NPs are solid colloidal systems wherein a chosen therapeutic agent is either dissolved, entrapped, encapsulated or adsorbed. These have recently emerged as chosen tools for treating varied cancers owing to their specific attribute of targeted delivery. This helps in circumventing the limitations of conventional chemotherapy like unwanted biodistribution, drug resistance and burden of undesirable systemic effects. Furthermore, their suitability to surface modification and precise engineering can make them versatile, as these can be tailored for long circulation, enhanced cellular internalization, better bioavailability and reduced toxicity (Chidambaram et al., 2011).

Our group has developed a novel nanoparticle enzyme encapsulation strategy that circumvents the limitation of immune responses to enzymes or PEG. Taking a cue from such findings, current research endeavours are aimed at delivering L-asparaginase via a PLGA-based nanoparticulate system, which is logically optimized by means of a well-established statistical tool of Box Behnken and its efficacy, as well as incidence of side effects were evaluated using an Ehrlich ascites tumor (EAT) model.

2. Materials and methods

2.1. Materials

L-asparaginase from *E. coli* was purified and provided ex gratia by PDC II Laboratory, National Institute of Immunology (NII) (New Delhi, India). Poly (lactic-co-glycolic acid) (PLGA) Resomer RG 503H, 50:50, 0.4 dL/g; MW 45,000, was provided as a gift by Evonik Industries AG (Essen, Germany). All the required chemicals were obtained from Sigma Aldrich (Mumbai, India). All were of high quality and HPLC grade. Double-distilled water was used throughout the experimentation. For evaluation of the particle size and polydispersity index, Zetasizer Nano ZS, Malvern Instruments (Malvern, United Kingdom) was used. For microscopic evaluation and observation, scanning electron microscopy, SEM; Hitachi, S-3400N (Tokyo, Japan) and transmission electron microscopy, TEM; CM-10; Philips, (Amsterdam, Netherlands) were carried out.

2.2. Formulation of L-asparaginase polymeric nanoparticles

Double emulsion solvent evaporation technique was adopted for preparing polymeric nanoparticles as described by the researchers with some modifications (Yang, 2001; Mehanny et al., 2017). An addition of 150 μL of the L-ASN solution, amounting to approximately 20 IU, was made to 1.5 mL of a dichloromethane (DCM) solution containing 150 mg of PLGA and 0.075 mL of 10% Span 60. This was then emulsified using a probe sonicator for a window of 15 s in an ice bath, resulting in the formation of o/w primary emulsion. The resulting solution was then added dropwise to 5 mL of a 1% PVA solution containing 5% Tween 80 and sonicated for 15 s to form the w/o/w secondary emulsion. Organic solvent was eliminated by constant stirring for 3 h until DCM was completely evaporated. The nanoparticles prepared were harvested and washed with five consecutive centrifugation and re-dispersion cycles at 4 °C in deionized water for 30 min at 15000 rpm. To ensure complete elimination of free drug and residual surfactants, nanoparticles were washed using deionized water. Further, dispersion of these particles in water followed by a

lyophilization period of 24 h, leading to the formation of freeze-dried, stable nanoparticles. For further characterization and optimization, the resulting nanoparticles were kept and maintained at a temperature of −20 °C and they were re-dispersed uniformly in normal saline with minimal shaking.

2.3. Optimization of formulation parameters using Box-Behnken design (BBD)

The independent variables chosen for the formulation of L-ASN-PN included L-asparaginase loading concentration (10–30%), PLGA-polymer concentration (150–200 mg) and sonication time (20–40 s). The particles were then evaluated with respect to the above independent variables of response surface methodology using Box-Behnken Design with Design Expert Software 8.0.7.1. Seventeen runs, as given by the design expert, were then performed in triplicate and the responses were evaluated in terms of dependent variables (particle size, polydispersity index and entrapment efficiency). For better understanding of the interaction between response variables and independent factors, response surface and contour plots were generated. Optimization of L-ASN-PN was carried out with the help of the predicted responses as given by the BBD software.

2.4. Particle size and PDI

Average particle size and polydispersity index (PDI) were determined by the dynamic light scattering (DLS) technique using a Zetasizer Nano ZS (Malvern, United Kingdom) and analysed by "DTS nano" software. Particle size and PDI were obtained using the 200-times-diluted formulation with the aqueous phase followed with vigorous shaking to attain approximately 100–250 kilo counts per second (Bhatt et al., 2013).

2.5. Scanning electron microscopy

Analysis of the optimized formulation for its shape and surface morphology was done using scanning electron microscopy, SEM; S-3400N (Tokyo, Japan) with help of previously reported procedures (Bhatt et al., 2013). A coating of gold sputter was made on the polymeric nanoparticles in order to make the surface more conductive and to obtain the images suggesting the morphology of the L-ASN-PN.

2.6. Transmission electron microscopy

Transmission electron microscopy (TEM) was employed for microscopically evaluating the optimized formulation. This was done using a TEM CM-10 (Amsterdam, Netherlands) (Kapoor et al., 2015). For evaluation, a drop of the formulation was put on a carbon-coated grid with 2% phospho-tungstic acid (PTA) and then was observed under TEM operated at 60–80 kV.

2.7. Entrapment efficiency

The entrapment efficiency of the L-ASN-PNs was calculated using the difference in the initial amount of protein used to prepare the nanoparticles and the protein present in the supernatant after centrifugation at 1500*g* at a temperature of 4 °C for a duration of 30 min. Bicinchoninic acid (BCA) protein assay was used for quantification of the protein content (Kapoor et al., 2015). Entrapment efficiency was determined using the following formula:

$$\text{Entrapment efficiency } (\%) = (T_i - T_f)100/T_i$$

where T_i is the total asparaginase used in the preparation of the particles, and T_f is the released asparaginase in the supernatant.

2.8. Asparaginase activity assay

Asparaginase activity was assayed using method described by Upadhyay et al. (2014). Briefly, reaction mixture consisted of 50 mM Tris-HCl (pH8.6) and 8.6 mM L-asparagine incubated at 37°C for 10 min. L-asparaginase enzyme solution(10 μg/ml) was added in reaction mixture and incubated at 37°C. Reaction was stopped by adding 1.5 M trichloroacetic acid at different time points and samples were centrifuged and used for estimation of released ammonia by Nessler's reagent using ammonium sulfate as standard. Time dependent release of ammonia was determined by taking OD measurements at 432 nm and linear range of ammonia release was found to be upto 30 min.An international unit (IU) of L asparaginase is defined as the amount of enzyme required to release one micromole of ammonia per min under the condition of the assay at saturating substrate concentration. Assays were run in triplicate.

2.9. In-vitro release studies

Release of protein from the L-ASN-PNs was determined by incubating the formulation in phosphate-buffered saline (PBS), pH 7, at 37 °C for a duration of 24 h. At time interval of 0.25, 0.50, 1, 2, 4, 8, 12, 18, 24 h, individual samples were withdrawn by centrifugation at 30,000*g* for 30 min at 4 °C, and the supernatant was replaced by fresh PBS. Release of protein was determined by BCA assay (Bhatt et al., 2013). The *in-vitro* release data was fitted into different kinetic models, such as zero-order and first-order, and the regression coefficient was determined in each case to find the best-fit model. Further, to describe the mechanism of release, the Korsmeyer-Peppas and Weibull models were applied and the release component (n), shape (α), and time parameter (Td) were calculated.

2.10. Radiolabelling of L-asparaginase polymeric nanoparticles

The prepared nanoparticles were radiolabelled with Technetium-99 m (^{99m}Tc) using a modified form of a previously reported method (Dunn et al., 1997). Briefly, pertechnetate (TcO^{4}-) (2 mCi) was reacted with stannous chloride (using 10% acetic acid), the pH was brought to 7.4 using 0.5 M sodium bicarbonate. Radiolabelling of the test formulation was done by adding a solution of Technetium-99 m at a concentration of 1 mg/mL and keeping it at room temperature for 10 min. The labelling efficiency was determined thereafter.

2.11. Radiolabelling efficiency

Instant thin-layer chromatography (ITLC) using silica gel impregnated strips was performed in order to determine the labelling efficiency. Different concentrations of the drug (200, 250, and 400 μL) were solubilized in 0.5 M sodium bicarbonate. A quantity of 150 μL stannous chloride solution (2 mL in 10% acetic acid) was dissolved in 100 mL of saline containing pertechnetate (^{99m}Tc-O_4), and the contents were then shaken gently (Singh et al., 2008). Filtration was performed with a 0.22 μm membrane filter. The filtered solution was kept for 10 min at room temperature after adjusting the pH to 6.5 using acetic acid. Labelling efficiency was established by ascending ITLC-silica gel (Gelman Science Inc., Ann Arbor, MI). Aliquots of 0.2–0.3 mL were retained on a 10 cm strip using acetone as the mobile phase. The solvent front was allowed to reach to a height of 8 cm from the base. The strip was divided into two halves, and radioactivity was determined with a gamma ray spectrometer (Type GRS23C, Electronics Corporation of India Limited, India).

2.12. Radiochemical purity

The presence of radio colloids was determined by a previously reported method by preparing an ITLC strip using pyridine: acetic acid: water (3:5:1:5) (Arulsudar et al., 2003). Reduced ^{99m}Tc- remains at the strip base, whereas ^{99m}Tc pertechnetate and labelled complexes drift with solvent front.

2.13. Tumor regression studies in EAT-bearing mice

2.13.1. Experimental animals

The study was approved by the Animal Ethics Committee of Jamia Hamdard, New Delhi, Registration Number (173/CPCSEA), Project Number (1048). Female albino mice weighing 25–30 g were obtained from the Central Animal House of the University and the experimental analysis was carried out in the Animal House of Institute of Nuclear Medicine and Applied Sciences, INMAS, DRDO. Animals were maintained in prescribed environmental conditions and fed with regular rodent diet with water and libitum (Jagetia and Rao, 2006). Ehrlich ascites tumor (EAT) cells were obtained from Division of Radiopharmaceuticals and Radiation Biology, Institute of Nuclear Medicine and Allied Sciences (INMAS, DRDO), Brig. SK Mazumdar Road, Delhi.

2.13.2. Experimental design and dosing

Animals were randomly divided into five groups with 5 mice in each group. Group-I served as **Normal Control** and received normal saline once daily orally throughout the study period; Group-II served as **EAC Control** which received EAT cells only (0.2 mL of $2 * 10^6$ cells/mice) (untreated); Group-III received standard drug, 5-FU (20 mg/kg) **EAC + 5-FU**; Group-IV was the Test group which received the L-ASN-PNs (200 mg/kg) **EAC + ASN-PN**. Group-V received neat drug **i.e.,** pure form of L-ASN, **EAC + Unformula ted/Neat** (200 mg/kg) (Samudrala et al., 2015).

2.13.3. Tumor regression studies

Intra-peritoneal injection of 0.2 mL of $2 * 10^6$ EAT cells/mice were administered in all groups except in Group I. 5-FU, L-ASN-PN and neat L-Asparaginase were injected daily via intra-venous route for 28 days to Groups III, IV and V, respectively. Tumor volume was measured using digital Vernier calipers and calculated according to the following formula (Padhi et al., 2015; Yehia et al., 2017):

$$\text{Tumor Volume } (V) = \text{Length}(L) * \text{Width } (W)^2/2$$

where

V = tumor volume
L = tumor length
W = tumor width

2.14. Biochemical studies and haematological studies

Blood samples from all animals were collected and taken for estimation of haematological parameters such as haemoglobin (Hb), red blood cell (RBC) count, and white blood cell (WBC) count and serum parameters such as serum alkaline phosphatase (SALP), serum glutamate pyruvate transaminase (SGPT), serum bilirubin, serum glutamate oxaloacetate transaminase (SGOT) and total protein (Thurnham et al., 2010; Duan and Li, 2013).

2.15. Gamma scintigraphy imaging studies

Radiolabelled ^{99m}Tc- L-ASN-PN complexes were used for imaging in tumor bearing mice weighing 25–30 g. The radiolabelled ^{99m}Tc- L-ASN-PN formulation was injected into tumor bearing mice through the tail vein. Imaging was done 1 h post administration using SPECT and the mice were fixed in place using surgical tape. Radio imaging was carried out, uptake of the ^{99m}Tc- L-ASN-PN formulation to the tumor was noted, and scintigraphy images of the animals at time intervals of 1 and 24 h were taken (Jain et al., 2009).

2.16. Statistics

Statistical analysis of the data was performed via one-way analysis of variance (ANOVA) followed by *t*-test using origin software 9.0 version; a value of $p < 0.05$ was considered significant ($n = 5$).

3. Results and discussion

3.1. Development and optimization of L-ASN-PN using BBD

L-ASN-PNs were prepared using a double emulsion evaporation technique and optimized by BBD. The effect of the various independent factors, such as L-asparaginase loading concentration (10–30%), PLGA polymer concentration (150–200 mg) and sonication time (20–40 sec), on the critical quality attributes of L-ASN-PNs was investigated. Optimum values of the different process variables were determined for the drug loading concentration (20%), the concentration of polymer (200 mg) and the sonication time (20 sec), and resulted in a particle size of 195 nm, a PDI of 0.21 and an EE of 80%.

Fig. 1(A) elucidates that when the drug loading concentration and polymer concentration was increased, particle size was also increased because the drug and polymer decrease the ultrasonication energy, resulting in particle agglomeration, and thereby increases the particle size. An increase in the sonication time resulted in a decreased particle size, which was due to the high sonication energy that results in a breakdown of the emulsion droplets and hence, attainment of small particle size (Das et al., 2011; Abdel-Hafez et al., 2014). The linear equation is as follows in which the terms A = L-asparaginase drug concentration, B = polymer concentration, and C = sonication time.

First Equation in terms of coded factors for R1 (Size) = +272.34 + 17.60*A-38.33*B + 40.98*C

The interaction of drug loading and polymer concentration on PDI can be seen in Fig. 1(B), which demonstrates that the drug loading and polymer concentration has an inverse effect on the PDI, i.e., with an increase in the above parameters PDI decreases. This could be attributed to the fact the higher concentration increases the formation of stabilized and small nanoparticles (Liu et al., 2007; Abdel-Hafez et al., 2018). Additionally, the interaction between the drug loading percentage and the sonication time was interpreted. Sonication time directly influences the PDI, as an increase in the sonication time decreases the PDI as it will break the bigger particles into smaller particles and hence, the monodispersity of the nanoparticles increases (Liu et al., 2007).

First Equation in terms of Coded Factors for R2 (PDI) = +0.29 + 0.029*A-0.044*B + 0.053*C.

Fig. 1(C) shows the interaction between the polymer concentration and the sonication time and its effect on entrapment efficiency. Sonication time increases the reduction in particle size, which leads to poor entrapment of the drug. Additionally, an increase in the polymer concentration solubilizes and entraps the drug more efficiently and hence, prevents the drug from leaching from the matrix (Jenning et al., 2000).

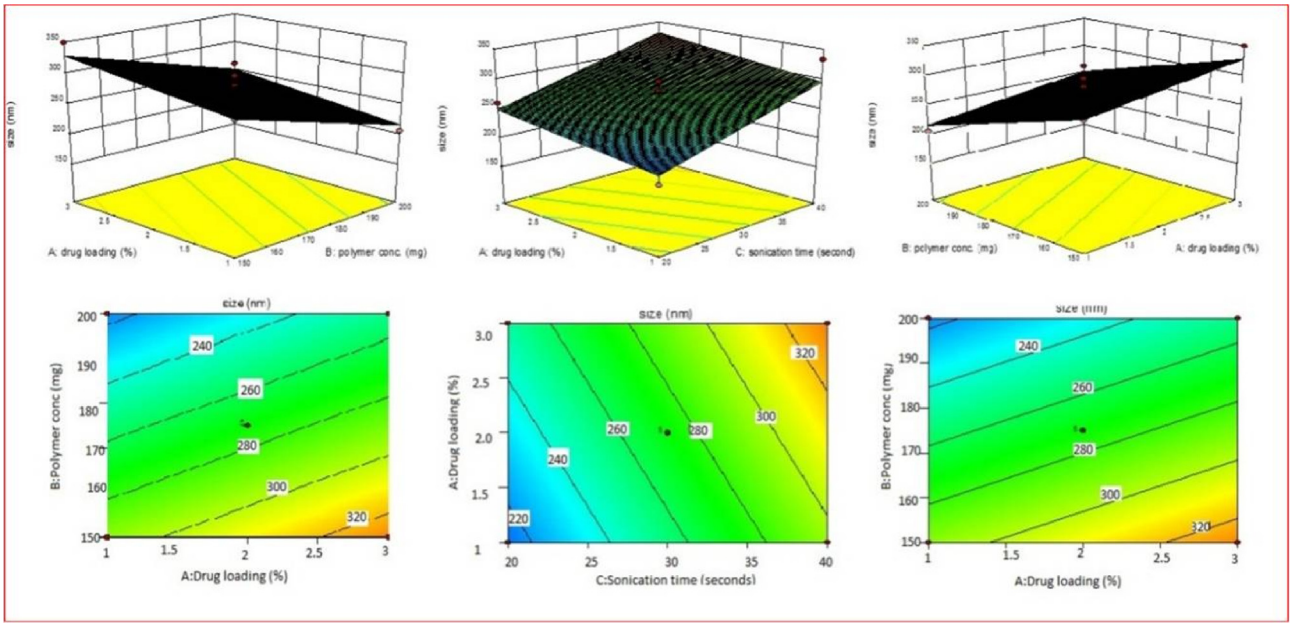

Fig. 1A. Effect of process parameters (drug loading, polymer concentration, and sonication time) on particle size.

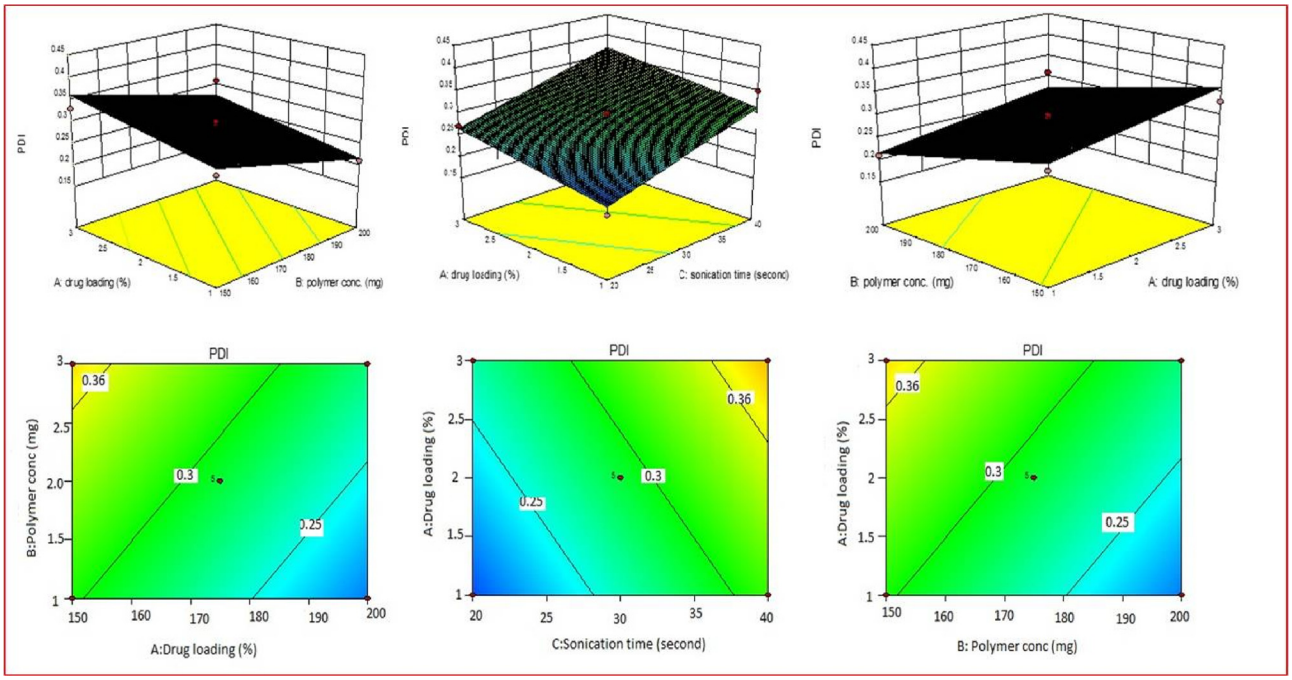

Fig. 1B. Effect of process parameters (drug loading, polymer concentration, and sonication time) on polydispersity index.

First Equation in terms of Coded Factors for R3 (%EE) = +76.86–0.68*A + 0.84*B − 10.03*C + 0.67*AB + 0.34*AC + 4.79*BC + 3.39*A^2 − 4.30*B^2 − 11.98*C^2.

Box-Behnken design (BBD) was used to explore and validate the outcome of varying process (independent) variables on the quality attributes (dependent variables) of the nanoparticles. It was evident that optimization of all of the independent factors was necessary in order to obtain the quality attributes of L-asparaginase (Safwat et al., 2016)

3.2. Particle size and PDI

The particle size and PDI of the optimized formulation was found to be 195 nm and 0.210, respectively. The results reveal that there is an even distribution of the particles throughout the formulation [Fig. 2(A)]. The optimized formulation of the L-ASN-PNs was found to be less than 200 nm, which is the optimal size for preventing recognition by the reticulo-endothelial system (RES) (Duval, 2002; El-Nagga et al., 2014; Soo et al., 2016), and hence, particles of this size exhibit longer half-life. Additionally, The higher anti-

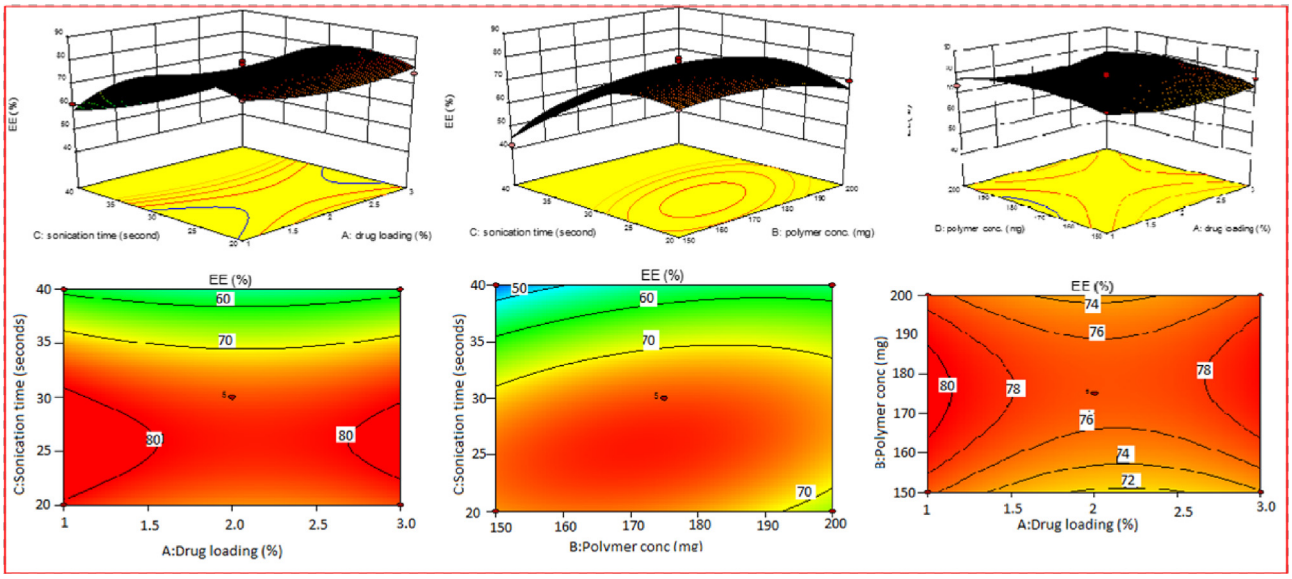

Fig. 1C. Effect of process parameters (drug loading, polymer concentration, and sonication time) on entrapment efficiency.

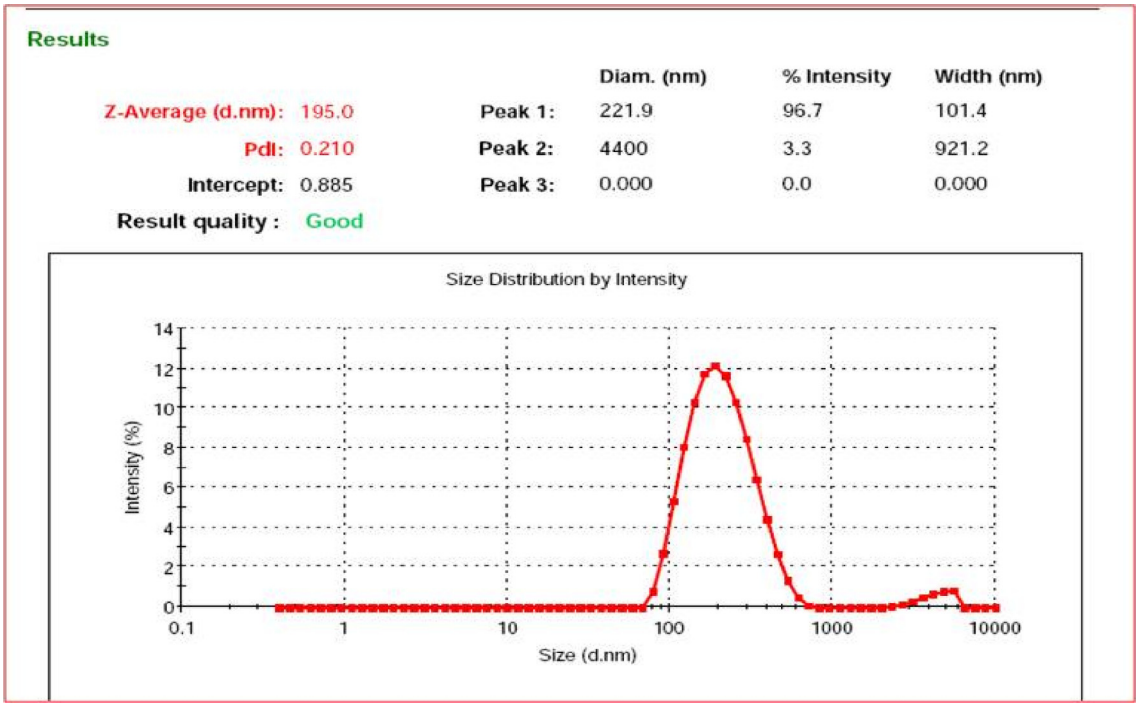

Fig. 2A. Particle size of the optimized formulation.

tumor activity of the L-ASN-PNs can also be attributed to their smaller size which could circumvent destruction by antibodies leading to increased availability at tumor sites.

3.3. TEM, SEM, and entrapment efficiency

Optimized particles were found to be in the range of 140–160 nm by TEM, which was in accordance with the results obtained from zetasizer analysis [Fig. 2B(i)]. Additionally, SEM images showed that the nanoparticles possessed a spherical and smooth surface [Fig. 2B(ii)]. Entrapment efficiency of the protein in polymer matrix was 80.23 ± 3.6%, which was significantly greater than previously reported PLGA nanoparticles (4.8%) and PEGylated L-ASN (48.6%) (Gaspar et al., 1998; Li et al., 2001).

3.4. Asparaginase activity assay

The specific activity of refolded, purified asparaginase as determined by the release of ammonia over a period of time up to 30 min using UV absorbance at 432 nm was akin to commercial asparaginase (190 IU/mg).

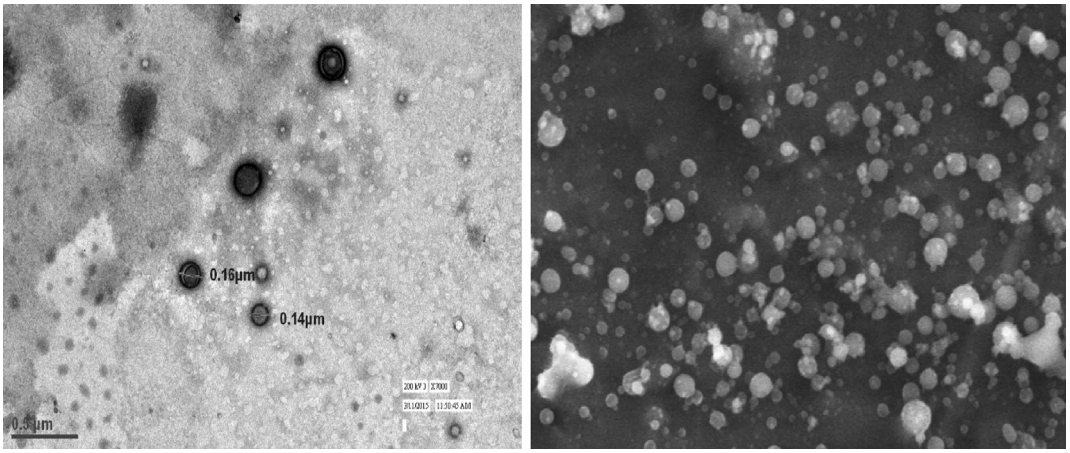

Fig. 2B. (Bi)Transmission electron microscopy and (Bii) Scanning electron microscopy images show a clear view of the entrapment of drug encapsulated into the polymer with particles ranging from 140 to 160 nm.

3.5. In-vitro release of L-ASN-PNs

In vitro release study of L-ASN-PNs showed continuous, slow release for over 24 h. The percentage of cumulative drug release was determined to be 80.23% ± 3.675% (n = 3) and is shown in Fig. 3. This continuous slow release over a period of time would help maintain the desired therapeutic concentration for a prolonged time and would reduce the frequency of administration. The protein activity for the *in-vitro* release samples was calculated by the asparaginase activity assay for a time period of 30 min and the protein activity was found to be 190 IU/mg (Upadhyay et al., 2014).

The *in-vitro* data was fitted into different kinetic models and the fitting parameters were determined (Table 1). The Higuchi model was found to be the best-fit model (R^2 = 0.9718), followed by the first order, which also showed a similar regression coefficient of 0.971. The mechanism of L-asparaginase release from PLGA nanoparticles was further analysed using the Korsmeyer-Peppas and Weibull models. The release component was obtained from the slope of the curve of log time vs. log % cumulative drug release.

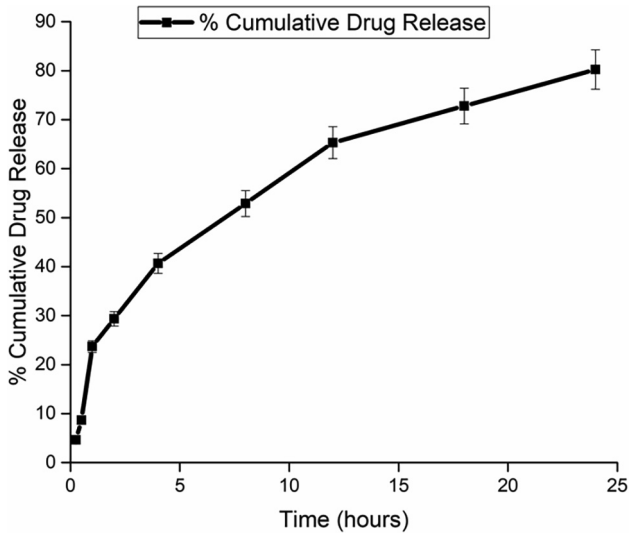

Fig. 3. *In-Vitro* release of L-ASN-PNs. The drug release behaviour of L-ASN-PN was investigated, and found that the relative burst drug releases at the initial stage and is followed by sustained release over 24 h with a cumulative 80.23% ± 3.675 of drug released.*Error bars are presented as mean ± S.E.M.

n value of 0.498 was obtained upon fitting the curve to the power law. Further, on analysing the Weibull model, the shape parameter, b = 0.581, was obtained, indicating a parabolic curve with a steeper initial slope than is consistent with the exponent. The time parameter Td was also calculated ($\alpha = Td^{\beta}$) and found to be 11.38, which defines the time (in hours) taken to release 63.2% of the protein.

The mathematical release modelling of the *in vitro* data revealed that the protein release followed both the Higuchi and first order kinetic model. This clearly indicates concentration dependent release and is primarily seen in the case of a PLGA porous matrix [40]. Further, n and b values of 0.498 and 0.581, respectively, indicated Fickian diffusion of asparaginase from the PLGA matrix (Dash et al., 2010). The time parameter (Td) showed that the 63.2% of asparaginase released from the matrix in 11.38 h, which indicated sustained release of the protein from the nanoparticles, which is essential for maintaining the therapeutic concentration.

3.6. Radiolabelling of L-ASN-PN

The labelling efficiency of the L-ASN-PNs with ^{99m}Tc was evaluated by instant thin layer chromatography (ITLC) using ITLC-SG mini strips and was found to be 99.8% efficient, and the occurrence of radio colloids was found to be > 1%. The radiolabelled nanoparticles were 96% to 98% stable in phosphate-buffered saline (pH 7.4) even after 24 h of labelling.

3.7. In-vivo tumor regression studies

The current study used an EAT model to evaluate the antitumor effect of the developed L-ASP-PNs since EAT is an undifferentiated, highly transplantable, rapidly proliferating and highly malignant tumor and is highly employed for finding the efficacy of PLGA nanoparticle-encapsulated cytotoxic drugs (Dash et al., 2010).

The initial 7 days of the study were required to establish a measurable tumor. The treatments were started from Day 7 to Day 30. The mice were sacrificed after 1 h of the last dose. No tumor initiation or treatment in Group I (Normal Control) was observed. In Fig. 4, it is seen that Group II (EAC Control) which had tumor induction but did not receive any drug and therefore, showed a continuous increase in tumor volume at all time points (14th, 21st and 30th Day). The group III (EAC + 5-FU) which was given standard care of therapy, 5-FU showed a reduction in tumor volume at days 14th, 21st and 30th . This reduction was comparable to the one obtained in Group V (EAC + Unformulated/Neat) which received

Table 1
Model fitting parameters. R is the regression coefficient; n is the release component; α and β are the time and shape constant; and Td is the time parameter.

Zero Order R^2	First Order R^2	Higuchi R^2	Korsmeyer Peppas		Weibull			
			R^2	n	R^2	A	B	Td (hrs)
0.8679	0.971	0.9718	0.97	0.498	0.993	4.07	0.58	11.38

the neat drug, and it was found to be lesser in the group IV that received the formulation (EAC + L-ASN-PN). Furthermore, it could be deduced that the group treated with L-ASN-PN showed comparatively slower tumor growth than the group treated with the 5-FU as well as the unformulated or the neat drug.

The effect of the L-ASN-PNs and 5-FU was evaluated in EAT tumor-bearing mice in terms of body weight, tumor volume and survival rate. Significant reductions were observed in both groups compared to the 5-FU group for tumor volume. L-ASN-PNs slowed tumor progression by 51.15% compared to the 5-FU group. These results were compared with the standard treatment drug 5-FU, which was found to be 15.86% (Fig. 4). The treatment with L-ASP-PNs was able to control body weight and tumor volume, which could be attributed to the encapsulation of L-asparaginase with PLGA, which halted progression of the tumor growth, and the cells were unable to proliferate further.

The survival rate of mice for a period of 30 days was found to be 20% for Group IV, 12% for Group III and 8% for Group V.

The reliable criterion for evaluating an anti-tumor drug is the ability to prolong the lifespan of a tumor-bearing animal model (Sriram et al., 2010). The untreated EAT control group mice showed decreased life span and increased WBC levels due to tumor progression. However, EAT-bearing mice treated with L-ASP-PNs showed an increased lifespan and suppressed tumor progression at doses of 200 mg/kg.

3.8. Effect of ASP-PNs on haematological parameters

EAT-bearing mice showed declined levels of Hb, RBCs, monocytes, and neutrophils and increased levels of WBCs and lymphocytes compared to the normal control and EAC control. EAT-bearing mice treated with L-ASP-PNs (200 mg/kg) and 5-FU (20 mg/kg) significantly ($p < 0.05$) inhibited the level of WBCs, lymphocytes and improved the levels of haemoglobin, RBCs, monocytes and neutrophils, as shown in Table 2(A). The treatment with plain L-ASN solution caused a marked fall in the WBCs, monocytes, neutrophils and lymphocytes that were significantly

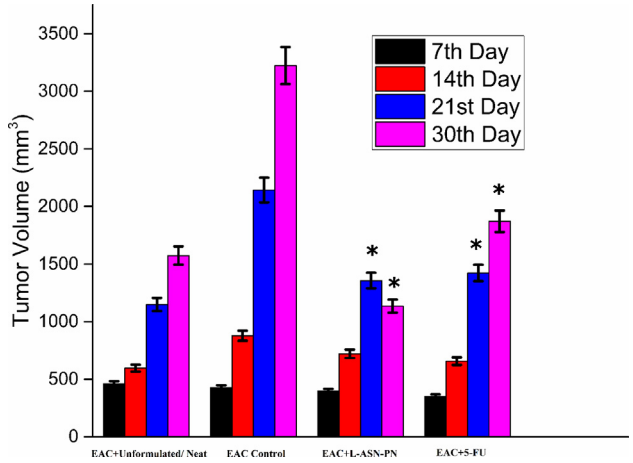

Fig. 4. Assessment of tumor volume for 30 days in a tumor regression model. Error bars are presented as mean ± S.E.M and *$p < 0.05$ statistically significant data.

increased due to the presence of tumor (as seen in EAC Control Group). This is a common phenomenon observed during chronic illness owing to the body's defence mechanism. However, when the tumor bearing mice were treated with plain L-ASN solution, a marked fall in the said parameters was observed which was attributed to the inherent toxic non-specific nature of L-ASN which caused cell death of the healthy fast-growing cells. In contrast, when L-ASN was incorporated in the PLGA nanoparticles and administered to the group (EAC + L-ASN-PN), the release of the free L-ASN was minimized, thereby preventing any detrimental effect on blood parameters. Hence, similar level was observed between the tumor bearing mice with no treatment and the group treated with L-ASN-NPs, indicating the ability of the nanoparticles to protect the drug and prevent its off-site release (Gupta et al., 2000).

3.9. Effect of ASP-PNs on serum parameters

EAT untreated mice and native L-ASN treated mice demonstrated increased level of SGOT, SGPT, SALP and total bilirubin compared to untreated controls. However, EAT-bearing mice treated with ASP-PNs (200 mg/kg) and 5-FU (20 mg/kg) showed significantly ($p < 0.05$) decreased levels of serum SGOT, SGPT, SALP, shown in Table 2(B). The parameters of groups in Table 2(B) were statistically significant in which $p < 0.05$. Thus, the tumor regression as well as the decreased concentration of native L-ASNs circulating in systemic circulation can be attributed to a higher encapsulation of L-asparaginase into PLGA polymeric nanoparticles (Moola et al., 1994). Also, it has been seen that L-asparaginase when given in an unformulated or neat form is responsible for hyperbilirubinemia. This is also corroborated in our studies where the neat drug has resulted in increased levels of SGOT, SGPT and SALP and while the strategy of encapsulation has successfully reduced the pronounced levels of SGOT, SGPT and SALP (Vora et al., 2006).

3.10. Gamma scintigraphy studies

Qualitative drug retention at the tumor site was determined by gamma scintigraphy with intravenous administration of the L-ASN-PNs labelled with ^{99m}Tc at time intervals of 1 and 24 h for localization and retention at the tumor site as visualized by gamma camera imaging, shown in Fig. 5. It was found that the drug was retained at the tumor site for a period of 24 h following single dose administration. Thus, these data suggest that the nanoparticles can accumulate at the desired tumor site at therapeutic levels for prolonged duration.

4. Conclusion

Formulation of cancer chemotherapeutics has long remained a research challenge. It is more demanding if the anticancer moiety is a protein, as the formulation design might lead to the attenuation of biological efficacy due to a change in its conformation, which is vital to its anticancer activity. L-asparaginase in its native form is associated with numerous side effects such as jaundice, easy bleeding, chemotoxicity, and hepatotoxicity, which are primarily due to its quick systemic release and the presence of chemical cross-linkers. The proposed formulation circumvents the above

Table 2A
Assessment of L-Asparaginase PLGA nanoparticles on serum biochemistry.

S. No	Groups	Haemoglobin (mg/dL)	RBC (cells × 10^6/mm^3)	WBCs (cells × 10^6/mm^3)	Monocytes (cells × 10^4/mm^3)	Neutrophils (cells × 10^4/mm^3)	Lymphocytes (cells × 10^4/mm^3)
1	Normal Control	14.6 ± 0.25	4.8 ± 0.67	4.6 ± 0.16	0.3 ± 0.04	2.4 ± 0.14	5.9 ± 0.56
2	EAC Control	9.56 ± 0.18	3.5 ± 0.65	7.5 ± 0.26	0.07 ± 0.04	4.4 ± 0.19	3.9. ± 0.26
3	EAC + Unformulated/Neat	5.22 ± 0.24	2.69 ± 1.1	5.9 ± 0.34	0.04 ± 0.02	2.2 ± 0.47	2.3 ± 0.54
4	EAC + L-ASN-PN	8.11 ± 0.23*	3.0 ± 0.37*	6.89 ± 0.11*	0.06 ± 0.02*	3.85 ± 0.34*	3.1 ± 0.89*
5	EAC + 5-FU	4.89 ± 1.13*	2.68 ± 0.38*	4.85 ± 0.51*	0.035 ± 0.03*	2.74 ± 0.24*	2.5 ± 0.76*

All the data have been represented as mean ± S.E.M and *p < 0.05 statistically significant data.

Table 2B
Assessment of L-Asparaginase PLGA nanoparticles on liver enzymes.

S. No	Groups	SGOT (IU/L)	SGPT (IU/L)	SALP (IU/L)	Total Protein (mg/dL)
1	Normal Control	39.6 ± 1.06	30.4 ± 0.23	80.5 ± 0.12	9.2 ± 0.12
2	EAC Control	45.2 ± 0.56	49.6 ± 0.87	87.4 ± 0.23	11.1 ± 0.43
3	EAC + Unformulated/Neat	70.5 ± 0.35	77.6 ± 0.34	168.5 ± 1.3	17.4 ± 0.29
4	EAC + L-ASN-PN	58.2 ± 0.8*	51.6 ± 0.46*	102.8 ± 1.12*	13.5 ± 0.67*
5	EAC + 5-FU	65.8 ± 1.1*	60.3 ± 0.89*	110.2 ± 076*	14.9 ± 0.41*

*All the data have been represented as mean ± S.E.M and *p < 0.05 statistically significant data.

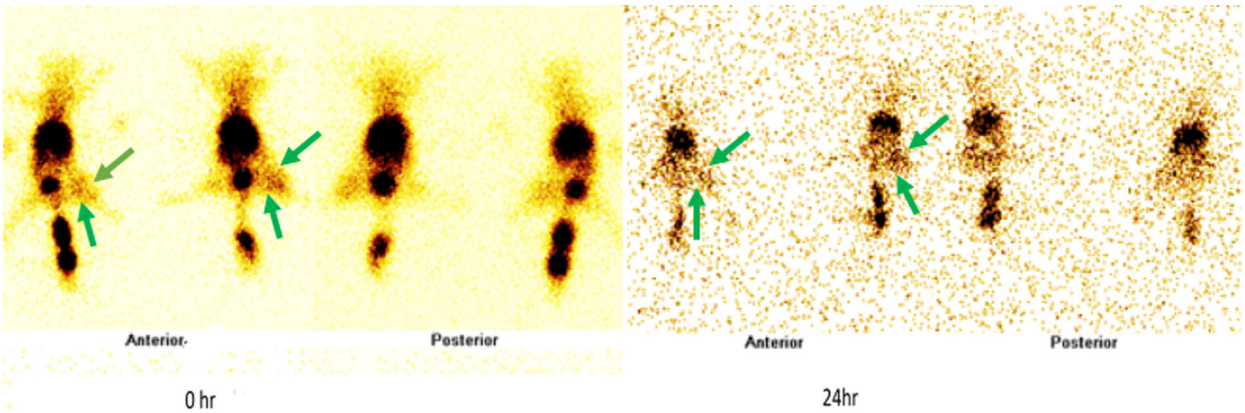

Fig. 5. Gamma scintigraphy images show a significant accumulation of drug at the tumor site.

caveats by ensuring a controlled delivery of the protein both *in vitro* (Higuchi kinetic model), at the site of action in an Ehrlich ascites tumor model and through gamma scintigraphy images for a period of 24 h. Additionally, the formulation parameters, such as particle size (195 nm ± 0.2 nm), PDI (0.2), and entrapment efficiency (80%), were appropriately tailored, assessed and optimized using a BBD. Administration of L-ASN-PN via intravenous route decreased the tumour progression by 51.15% when compared with the marketed formulation for cancer treatment. Conclusively, the formulation approach could be exploited as a platform for the delivery of other protein molecules and drug variants wherein maintaining the molecular conformation is a pre-requisite for the efficacy of the product while fulfilling the pharmaco-technical parameters for better anticancer effect.

Author Contributions

The experimental design was conceived by Zeenat Iqbal, Bibhu Prasad Panda. The experiments were performed by Manvi Singh, Nazia Hassan and Devina Verma. The statistical analysis was done by Pragya Thakur, Amulya Kumar Panda and Rakesh Kumar Sharma. Aamir Mirza and Sheikh Mansoor helped in original draft preparation. Salman H. Alrokayan, Haseeb A. Khan, Zeenat Iqbal and Parvaiz Ahmad helped in data analysis and revising the manuscript to present form.

Declaration of Competing Interest

The authors declare that they have no known competing financial interests or personal relationships that could have appeared to influence the work reported in this paper.

Acknowledgment

We deeply acknowledge the Animal House of Institute of Nuclear Medicine and Allied Sciences (INMAS, DRDO). The authors would like to extend their sincere appreciation to the Deanship of Scientific Research at King Saud University for funding the Research Group No. RGP-1435-066.

References

Abdel-Hafez, S.M., Hathout, R.M., Sammour, O.A., 2014. Towards better modeling of chitosan nanoparticles production: Screening different factors and comparing two experimental designs Available from Int. J. Biol. Macromol. 64, 334–340. https://doi.org/10.1016/j.ijbiomac.2013.11.041. DOI 10.1016/j.ijbiomac.2013.11.041.

Abdel-Hafez, S.M., Hathout, R.M., Sammour, O.A., 2018. Curcumin-loaded ultradeformable nanovesicles as a potential delivery system for breast cancer therapy. Colloids and Surfaces B: Biointerfaces 167, 63–72. Available from http://dx.doi.org/10.1016/j.colsurfb.2018.03.051.

Arulsudar, N., Subramanian, N., Mishra, P., Sharma, R.K., Murthy, R.S.R., 2003. Preparation, characterisation and biodistribution of 99mTc-labeled liposome encapsulated cyclosporine. Journal of drug targeting 11 (3), 187–196.

Bahreini, E., Aghaiypour, K., Abbasalipourkabir, R., Mokarram, A., Goodarzi, M., Saidijam, M., 2014. Preparation and nanoencapsulation of l-asparaginase ii in chitosan-tripolyphosphate nanoparticles and in vitro release study. Nanoscale Res. Lett. 9(1), 340. Available from http://dx.doi.org/10.1186/1556-276x-9-340.

Baskar, G., Chandhuru, J., Sheraz Fahad, K., Praveen, A.S., Chamundeeswari, M., Muthukumar, T., 2015. Anticancer activity of fungal l-asparaginase conjugated with zinc oxide nanoparticles. J. Mater. Sci.: Mater. Med. 26(1). Available from http://dx.doi.org/10.1007/s10856-015-5380-z.

Bhatt, P.C., Ahmad, M., Panda, B.P., 2013. Enhanced bioaccumulation of astaxanthin in *phaffia rhodozyma* by utilising low-cost agro products as fermentation substrate. Biocatalysis and Agricultural. Biotechnology 2 (1), 58–63. https://doi.org/10.1016/j.bcab.2012.11.002.

Brambilla, G., Parodi, S., Cavanna, M., Baldini, L., 1970. The immunodepressive activity of n-diazoacetylglycine amide in some transplantation systems. Transplantation 10(1), 100–105. Available from http://dx.doi.org/10.1097/00007890-197007000-00011.

Cedar, H., Schwartz, J.H., 1968. Production of L-asparaginase II by Escherichia coli. J. Bacteriol. 96 (6), 2043–2048.

Chidambaram, M., Manavalan, R., Kathiresan, K., 2011. Nanotherapeutics to overcome conventional cancer chemotherapy limitations. J. Pharm. Pharmaceut. Sci. 14 (1), 67. https://doi.org/10.18433/j30c7d.

Das, S., Ng, W.K., Kanaujia, P., Kim, S., Tan, R.B.H., 2011. Formulation design, preparation and physicochemical characterizations of solid lipid nanoparticles containing a hydrophobic drug: Effects of process variables. Colloids Surf. B Biointerfaces 88 (1), 483–489. https://doi.org/10.1016/j.colsurfb.2011.07.036.

Dash, S., Murthy, P.N., Nath, L., Chowdhury, P., 2010. Kinetic modeling on drug release from controlled drug delivery systems. Acta Pol Pharm 67 (3), 217–223.

Duan, X., Li, Y., 2012. Physicochemical characteristics of nanoparticles affect circulation, biodistribution, cellular internalization, and trafficking. Small 9(9-10), 1521–1532. Available from http://dx.doi.org/10.1002/smll.201201390.

Dunn, S.E., Kari, F.W., French, J., Leininger, J.R., Travlos, G., Wilson, R., Barrett, J.C., 1997. Dietary restriction reduces insulin-like growth factor i levels, which modulates apoptosis, cell proliferation, and tumor progression in p53-deficient mice. Cancer Res. 57 (21), 4667–4672.

Duval, M., 2002. Comparison of escherichia coli-asparaginase with erwinia-asparaginase in the treatment of childhood lymphoid malignancies: Results of a randomized european organisation for research and treatment of cancer––children's leukemia group phase 3 trial. Blood 99 (8), 2734–2739. https://doi.org/10.1182/blood.v99.8.2734.

El-Nagga, N.E.-A., El-Ewasy, S.M., El-Shweihy, N.M., 2014. Microbial l-asparaginase as a potential therapeutic agent for the treatment of acute lymphoblastic leukemia: The pros and cons. Int. J. Pharmacol. 10 (4), 182–199. https://doi.org/10.3923/ijp.2014.182.199.

Fishman, Y., Citri, N., 1975. L-asparaginase entrapped in liposomes: Preparation and properties. FEBS Lett. 60 (1), 17–20. https://doi.org/10.1016/0014-5793(75)80408-x.

Fu, C.H., Sakamoto, K.M., 2007. Peg-asparaginase. Expert Opin. Pharmacother. 8 (12), 1977–1984. https://doi.org/10.1517/14656566.8.12.1977.

Gaspar, M.M., Blanco, D., Cruz, M.E.M., José Alonso, M.A., 1998. Formulation of l-asparaginase-loaded poly(lactide-co-glycolide) nanoparticles: Influence of polymer properties on enzyme loading, activity and in vitro release. J. f Controlled Release 52(1-2), 53–62. Available from http://dx.doi.org/10.1016/s0168-3659(97)00196-x.

Gupta, M., Mazumder, U.K., Rath, N., Mukhopadhyay, D.K., 2000. Antitumor activity of methanolic extract of *cassia fistula* l. Seed against ehrlich ascites carcinoma. J. Ethnopharmacol. 72 (1–2), 151–156. https://doi.org/10.1016/s0378-8741(00)00227-0.

Jagetia, G.C., Rao, S.K., 2006. Evaluation of the antineoplastic activity of guduchi (tinospora cordifolia) in ehrlich ascites carcinoma bearing mice. Biol. Pharm. Bull. 29 (3), 460–466. https://doi.org/10.1248/bpb.29.460.

Jain, R., Zaidi, K.U., Verma, Y., Saxena, P., 2012. L-asparaginase: A promising enzyme for treatment of acute lymphoblastic leukiemia. People's J. Sci. Res. 5 (1), 29–35.

Jain, S., Dani, P., Sharma, R.K., 2009. Pharmacoscintigraphy: A blazing trail for the evaluation of new drugs and delivery systems. Critical Reviews™ in Therapeutic Drug Carrier Systems 26 (4), 373–426. https://doi.org/10.1615/critrevtherdrugcarriersyst.v26.i4.20.

Jenning, V., Thünemann, A.F., Gohla, S.H., 2000. Characterisation of a novel solid lipid nanoparticle carrier system based on binary mixtures of liquid and solid lipids. Int. J. Pharm. 199 (2), 167–177. https://doi.org/10.1016/s0378-5173(00)00378-1.

Kapoor, R., Harde, H., Jain, S., Panda, A.K., Panda, B.P., 2015. Downstream processing, formulation development and antithrombotic evaluation of microbial nattokinase. J. Biomed. Nanotechnol. 11 (7), 1213–1224. https://doi.org/10.1166/jbn.2015.2071.

Li, Y.-P., Pei, Y.-Y., Zhang, X.-Y., Gu, Z.-H., Zhou, Z.-H., Yuan, W.-F., Zhou, J.-J., Zhu, J.-H., Gao, X.-J., 2001. Pegylated plga nanoparticles as protein carriers: Synthesis, preparation and biodistribution in rats. J. Control. Release 71 (2), 203–211. https://doi.org/10.1016/s0168-3659(01)00218-8.

Liu, J., Hu, W., Chen, H., Ni, Q., Xu, H., Yang, X., 2007. Isotretinoin-loaded solid lipid nanoparticles with skin targeting for topical delivery. Int. J. Pharm. 328 (2), 191–195. https://doi.org/10.1016/j.ijpharm.2006.08.007.

Masetti, R., Pession, A., 2009. First-line treatment of acute lymphoblastic leukemia with pegasparaginase. Biologics: targets & therapy 3, 359.

Matsushima, A., Nishimura, H., Ashihara, Y., Yokota, Y., Inada, Y., 1980. Modification of *e. Coli* asparaginase with 2, 4-bis (o-methoxypolyethylene glycol)-6-chloro-s-triazine (activated peg2); disappearance of binding ability towards anti-serum and retention of enzymic activity. Chem. Lett. 9 (7), 773–776.

Mehanny, M., Hathout, R.M., Geneidi, A.S., Mansour, S., 2017. Studying the effect of physically-adsorbed coating polymers on the cytotoxic activity of optimized bisdemethoxycurcumin loaded-plga nanoparticles. J. Biomed. Mater. Res. Part A 105 (5), 1433–1445. https://doi.org/10.1002/jbm.a.36028.

Moola, Z.B., Scawen, M.D., Atkinson, T., Nicholls, D.J., 1994. Erwinia chrysanthemi l-asparaginase: Epitope mapping and production of antigenically modified enzymes. Biochem. J 302 (3), 921–927. https://doi.org/10.1042/bj3020921.

Padhi, S., Mirza, M.A., Verma, D., Khuroo, T., Panda, A.K., Talegaonkar, S., Khar, R.K., Iqbal, Z., 2015. Revisiting the nanoformulation design approach for effective delivery of topotecan in its stable form: An appraisal of its in vitro behavior and tumor amelioration potential. Drug Delivery 23 (8), 2827–2837. https://doi.org/10.3109/10717544.2015.1105323.

Pieters, R., Hunger, S.P., Boos, J., Rizzari, C., Silverman, L., Baruchel, A., Goekbuget, N., Schrappe, M., Pui, C.-H., 2010. L-asparaginase treatment in acute lymphoblastic leukemia. Cancer 117 (2), 238–249. https://doi.org/10.1002/cncr.25489.

Safwat, S., Hathout, R.M., Ishak, R.A., Mortada, N.D., 2016. Augmented simvastatin cytotoxicity using optimized lipid nanocapsules: A potential for breast cancer treatment. J. Liposome Res. 27 (1), 1–10. https://doi.org/10.3109/08982104.2015.1137313.

Samudrala, P.K., Augustine, B.B., Kasala, E.R., Bodduluru, L.N., Barua, C., Lahkar, M., 2015. Evaluation of antitumor activity and antioxidant status of Alternanthera brasiliana against Ehrlich ascites carcinoma in Swiss albino mice. Pharmacognosy Res. 7(1), 66–73. Available from DOI: 10.4103/0974-8490.147211.

Singh, R., Tian, B., Kostarelos, K., 2008. Artificial envelopment of nonenveloped viruses: Enhancing adenovirus tumor targeting in vivo. FASEB J. 22 (9), 3389–3402. https://doi.org/10.1096/fj.08-103275.

Soo, E., Thakur, S., Qu, Z., Jambhrunkar, S., Parekh, H.S., Popat, A., 2016. Enhancing delivery and cytotoxicity of resveratrol through a dual nanoencapsulation approach. J. Colloid Interface Sci. 462, 368–374. https://doi.org/10.1016/j.jcis.2015.10.022.

Sriram, M.I., Kanth, S.B.M., Kalishwaralal, K., Gurunathan, S., 2010. Antitumor activity of silver nanoparticles in dalton's lymphoma ascites tumor model. Int. J. Nanomed. 5, 753.

Teodor, E., Litescu, S.-C., Lazar, V., Somoghi, R., 2009. Hydrogel-magnetic nanoparticles with immobilized l-asparaginase for biomedical applications. J. Mater. Sci. - Mater. Med. 20 (6), 1307–1314. https://doi.org/10.1007/s10856-008-3684-y.

Thurnham, D.I., McCabe, L.D., Haldar, S., Wieringa, F.T., Northrop-Clewes, C.A., McCabe, G.P., 2010. Adjusting plasma ferritin concentrations to remove the effects of subclinical inflammation in the assessment of iron deficiency: A meta-analysis. The American Journal of Clinical Nutrition 92 (3), 546–555. https://doi.org/10.3945/ajcn.2010.29284.

Upadhyay, A.K., Singh, O.A., Mukherjee, K.J., Panda, K.J., 2014. Refolding and purification of recombinant l-asparaginase from inclusion bodies of e. Coli into active tetrameric protein. Front. Microbiol. 5. Available from http://dx.doi.org/10.3389/fmicb.2014.00486.

Uren, J.R., Hargis, B.J., Beardsley, P., 1982. Immunological and pharmacological characterization of poly-dl-alanyl-modified *erwinia carotovora* l-asparaginase. Cancer Res. 42 (10), 4068–4071.

Vora, A.D., Pai, V.R., Kumar, P., Banavali, S., Nair, R., Kurkure, P., Parikh, P.M., 2006. Profound hyperbilirubinemia during induction of adult acute lymphoblastic leukemia: Capping l-asparaginase dose to 10,000 units attenuates it without compromising remission rate. Blood 108 (11), 4531. https://doi.org/10.1182/blood.v108.11.4531.4531.

Wang, N., Wu, X.S., Li, J.K., 1999. A heterogeneously structured composite based on poly (lactic-co-glycolic acid) microspheres and poly (vinyl alcohol) hydrogel nanoparticles for long-term protein drug delivery. Pharm. Res. 16 (9), 1430–1435.

Wileman, T.E., Foster, R.L., Elliott, P.N.C., 1986. Soluble asparaginase-dextran conjugates show increased circulatory persistence and lowered antigen reactivity. J. Pharm. Pharmacol. 38 (4), 264–271. https://doi.org/10.1111/j.2042-7158.1986.tb04564.x.

Wolf, M., Wirth, M., Pittner, F., Gabor, F., 2003. Stabilisation and determination of the biological activity of l-asparaginase in poly(d, l-lactide-co-glycolide) nanospheres. Int. J. Pharm. 256 (1–2), 141–152. https://doi.org/10.1016/s0378-5173(03)00071-1.

Yang, Y., 2001. Morphology, drug distribution, and in vitro release profiles of biodegradable polymeric microspheres containing protein fabricated by double-emulsion solvent extraction/evaporation method. Biomaterials 22(3), 231–241. Available from http://dx.doi.org/10.1016/s0142-9612(00)00178-2.

Yehia, R., Hathout, R.M., Attia, D.A., Elmazar, M.M., Mortada, N.D., 2017. Anti-tumor efficacy of an integrated methyl dihydrojasmonate transdermal microemulsion system targeting breast cancer cells: In vitro and in vivo studies. Colloids Surf., B 155, 512–521. https://doi.org/10.1016/j.colsurfb.2017.04.031.